FOI-R--1404--SE
November 2004
ISSN 1650-1942

Base data report

Henrik Claésson

A Boundary Element Code with implemented equations for Static Electric Fields

Systems Technology
SE-172 90 Stockholm

SWEDISH DEFENCE RESEARCH AGENCY

Systems Technology
SE-172 90 Stockholm

FOI-R--1404--SE

November 2004

ISSN 1650-1942

Base data report

Henrik Claésson

A Boundary Element Code with implemented equations for Static Electric Fields

Issuing organization	Report number, ISRN	Report type
FOI – Swedish Defence Research Agency Systems Technology SE-172 90 Stockholm	FOI-R--1404--SE	Base data report
	Research area code 43 Underwater Sensors	
	Month year November 2004	**Project no.** E6058
	Sub area code 43 Underwater Sensors	
	Sub area code 2	

Author/s (editor/s)	Project manager
Henrik Claésson	Henrik Claésson
	Approved by Monica Dahlén
	Sponsoring agency Swedish Armed Force
	Scientifically and technically responsible Henrik Claésson

Report title

A Boundary Element Code with Implemented Equations for Static Electric Fields

Abstract (not more than 200 words)

In this report we give the theory for a boundary element code, electrostatic integral equations and the numerical implementation. We show example of validation conducted against an analytical solution as a function of the surface discretization, where we see the expected convergence, as well as a comparision of the solutions between a commercial boundary element code and our for a more advance geometry, which result in similar solutions.

Keywords

boundary element code, integral equations, static electric field, Lagrangian basis function, triangular elements

Further bibliographic information	Language English
ISSN 1650-1942	**Pages** 11 p.
	Price acc. to pricelist

Utgivare Totalförsvarets Forskningsinstitut - FOI Systemteknik 172 90 Stockholm	**Rapportnummer, ISRN** FOI-R--1404--SE	**Klassificering** Underlagsrapport
	Forskningsområde 4. Ledning, informationsteknik och sensorer	
	Månad, år November 2004	**Projektnummer** E6058
	Delområde 43 Undervattenssensorer	
	Delområde 2	

Författare/redaktör Henrik Claésson	**Projektledare** Henrik Claésson
	Godkänd av Monica Dahlén
	Uppdragsgivare/kundbeteckning Försvarsmakten
	Tekniskt och/eller vetenskapligt ansvarig Henrik Claésson

Rapportens titel (i översättning)

En randelementkod med implementerade ekvationer för statiska elektriska fält

Sammanfattning (högst 200 ord)

I denna rapport beskrivs arbetet som gjorts med att ta fram teori för randelementkod, de elektrostatiska integralekvationerna samt implementeringen av dessa. Vi ger också ett par exempel på validering av implementeringen, dels mot en analytisk lösning som funktion av diskretiseringen av ytan, där vi ser den förväntade konvergensen, samt dels som en jämförelse av lösningen från en kommersiell randelementkod på en mer avancerad geometri, där vi ser liknande lösningar.

Nyckelord

randelementkod, integralekvationer, statiska elektriska fält, Lagrange basfunktioner, triangulära element

Övriga bibliografiska uppgifter	**Språk** Engelska
ISSN 1650-1942	**Antal sidor:** 11 s.
Distribution enligt missiv	**Pris: Enligt prislista**

1. Background

The static electric field caused by corrosion currents exists around most ships. It is important to study the possibility to reduce the electric signature by transmitting current from anodes to the hull, since there exist sea-mines that use the static electric field as trigger. A system that would control the electric signature would consist of current transmitting anodes and hull-mounted potential measuring electrodes. The importance of accurate modeling a complex surface geometry is evident for electric potential measurements close to such surface. In a physical scale model experiment [1], where current transmitting anodes and potential measuring sensors were mounted onto the hull, a commercial boundary element code, using the full geometry, predicted the measured potential accurately.

The implemented boundary element code is intended to be used in the research on active reduction of the corrosion and static electric signatures as a forward model in an inverse solver or a regulator.

2. Introduction

The relation between the potential and the normal current density on a surface could be expressed as an integral equation. In the Dirichlet problem the potential on the surface ∂B is given and in the Neumann problem the normal current density on the surface is given. Two different types of problems are associated with these boundary conditions, the interior and the exterior problem. The discretization of the surface into faces is usually done with curved triangular or quadrilateral faces approximated by some set of basis function defined by its node points. Onto these faces the seeked density function is expanded into another set of basis function, chosen in order to preserve some characteristics of the density function such as continuity, continuous tangential derivative etc. From this discretization it is possible to derive a set of linear equations that solve the integral equation, i.e. calculate the coefficients of the chosen set of basis functions.

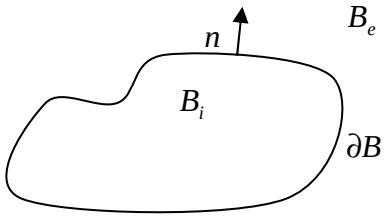

Figure 1. The interior domain B_i enclosed by the surface ∂B with the unit normal pointing into the exterior domain B_e.

In our application the surface ∂B is the hull of a ship and thus we are interested in the exterior domain B_e corresponding to the water region. The work presented here is a formulation and implementation of the exterior integral equations for calculating the electric potential field resulting from a Dirichlet or a Neumann boundary condition using a boundary element approach. The surface is defined by curved triangular faces, where an isoparametric expansion is applied, i.e. the surface curvature and the density function on the surface ∂B is discretized into the same set of basis function. We have chosen a Lagrangian expansion, which is interpolatory within each face, where the continuity of the density functions is

enforced by choosing the node points to be the collocation points. The theory is derived for a general order of Lagrangian polynomial and implemented for a quadratic expansion.

3. Theory

3.1. Potential Theory

From the existence theorem of harmonic functions we know that for a given potential or normal derivative of the potential on a Liapunov[1] surface, there exist a unique potential in the interior domain B_i that assume the given values on the surface. For the exterior domain B_e the theorem holds provided that we have $\boldsymbol{O}(r^{-1})$ behavior of the potential field as $r \to \infty$. The derived equations are valid for the exterior domain. We assume that all sources are located on a perfectly conducting surface and that the exterior domain is source free, i.e. the divergence of the current density vector is zero

$$\nabla \cdot \mathbf{J}(\mathbf{r}) = 0 \; ; \qquad \mathbf{r} \in B_e \, . \tag{1}$$

For a homogeneous conducting medium, the postulate of irrotational static electric fields imply that

$$\nabla \times \mathbf{J}(\mathbf{r}) = 0 \; ; \qquad \mathbf{r} \in B_e \, . \tag{2}$$

The current density can thus be written as the gradient of a scalar field $\phi(\mathbf{r})$, known as the current potential,

$$\mathbf{J}(\mathbf{r}) = -\nabla \phi(\mathbf{r}) \, ; \qquad \mathbf{r} \in B_e \, . \tag{3}$$

Substituting (3) into equation (1) yield a Laplacian equation in $\phi(\mathbf{r})$

$$\Delta \phi(\mathbf{r}) = 0 \, ; \qquad \mathbf{r} \in B_e \, . \tag{4}$$

Since all the sources are located on ∂B it follows that $\phi(\mathbf{r})$ has an $\boldsymbol{O}(r^{-2})$ behavior as $r \to \infty$. The electric potential $V(\mathbf{r})$ relates to the current potential as

$$V(\mathbf{r}) = \frac{\phi(\mathbf{r})}{\sigma} \, ; \qquad \mathbf{r} \in B_e \, , \tag{5}$$

where σ is the conductivity of the medium in the exterior domain.

[1] A Liapunov surface is defined by $\cos^{-1}(n_{\mathbf{r}} \cdot n_{\mathbf{r}'}) \le D\left|\mathbf{r} - \mathbf{r}'\right|^{\nu}$; $0 < \nu \le 1$, $D > 0$, which is slightly stronger than C^1, but weaker than C^2.

3.2. Integral formulation

The current potential field is written either as a single layer representation (6) or as a double layer representation (7)

$$\phi(\mathbf{r}) = \int_{\partial B} g(\mathbf{r},\mathbf{r}')\gamma(\mathbf{r}')dr'; \qquad \mathbf{r} \in B_e \tag{6}$$

$$\phi(\mathbf{r}) = \int_{\partial B} \frac{\partial g(\mathbf{r},\mathbf{r}')}{\partial n}\mu(\mathbf{r}')dr'; \qquad \mathbf{r} \in B_e \ , \tag{7}$$

where $g(\mathbf{r},\mathbf{r}')$ is the solution to the fundamental Laplacian equation

$$-\Delta g(\mathbf{r},\mathbf{r}') = \delta(\mathbf{r},\mathbf{r}'), \tag{8}$$

and $\gamma(\mathbf{r}')$ and $\mu(\mathbf{r}')$ are density functions. The nomenclature for the normal derivative with respect to $\mathbf{r}$ is written as $n\cdot\nabla = \frac{\partial}{\partial n}$ and with respect to $\mathbf{r}'$ as $n'\cdot\nabla' = \frac{\partial}{\partial n'}$. In a homogenous medium the fundamental solutions is defined by

$$g(\mathbf{r},\mathbf{r}') = \frac{1}{4\pi|\mathbf{r}-\mathbf{r}'|} \ , \tag{9}$$

which imply that

$$\frac{\partial g(\mathbf{r},\mathbf{r}')}{\partial n} = \frac{\partial g(\mathbf{r}',\mathbf{r})}{\partial n'}. \tag{10}$$

The type of representation is chosen so that a Fredholm integral equation (FIE) of a second order is obtained. It is well known that a second order FIE is preferable to a first order FIE since the kernel matrix is diagonal heavy and thus well conditioned.

3.3. Exterior Neumann problem

With the normal derivative of the current potential $\frac{\partial}{\partial n}\phi(\mathbf{r})$ given on ∂B, we have chosen a single layer representation of the current potential field as [2],

$$\phi(\mathbf{r}) = \int_{\partial B} g(\mathbf{r},\mathbf{r}')\gamma(\mathbf{r}')dr'; \qquad \mathbf{r} \in B_e. \tag{11}$$

By differentiation of equation (11) we obtain

$$\nabla\phi(\mathbf{r}) = \int_{\partial B} \nabla g(\mathbf{r},\mathbf{r}')\gamma(\mathbf{r}')dr'; \qquad \mathbf{r} \in B_e \tag{12}$$

$$\frac{\partial}{\partial n}\phi(\mathbf{r}) = \int_{\partial B} \frac{\partial g(\mathbf{r},\mathbf{r}')}{\partial n}\gamma(\mathbf{r}')dr'; \qquad \mathbf{r} \in B_e. \tag{13}$$

As we move the field point in equation (13) to the surface,

we obtain a FIE of the second kind for $\gamma(\mathbf{r}')$ in terms of $\frac{\partial}{\partial n}\phi(\mathbf{r})$ as

$$\frac{\partial}{\partial n}\phi(\mathbf{r}) = \int_{\partial B} \frac{\partial g(\mathbf{r},\mathbf{r}')}{\partial n}\gamma(\mathbf{r}')dr' - \tfrac{1}{2}\gamma(\mathbf{r}); \qquad \mathbf{r} \in \partial B. \tag{14}$$

With the source density $\gamma(\mathbf{r}')$ known we may calculate the electric potential $V(\mathbf{r})$ utilizing equations (11) and (5) and the current density $\mathbf{J}(\mathbf{r})$ from equation (12) and (3). The potential on the surface is calculated just outside of ∂B using (11), utilizing that the potential is continuous across an interface.

3.4. Exterior Dirichlet problem

With the current potential $\phi(\mathbf{r})$ given on the surface, we have chosen to represent the current potential field with a double layer approach as [2]

$$\phi(\mathbf{r}) = \int_{\partial B} \frac{\partial g(\mathbf{r},\mathbf{r}')}{\partial n'}\mu(\mathbf{r}')dr' + \phi_\infty; \qquad \mathbf{r} \in B_e, \tag{15}$$

where ϕ_∞ is the current infinity potential. As we move the source point in equation (15) to the surface we obtain a FIE of the second kind for $\mu(\mathbf{r}')$ in terms of $(\phi(\mathbf{r}) - \phi_\infty)$ as

$$\phi(\mathbf{r}) - \phi_\infty = \int_{\partial B} \frac{\partial g(\mathbf{r},\mathbf{r}')}{\partial n'}\mu(\mathbf{r}')dr' + \tfrac{1}{2}\mu(\mathbf{r}); \qquad \mathbf{r} \in \partial B. \tag{16}$$

To ensure an $\boldsymbol{O}(r^{-2})$ behavior at infinity, the current potential must fulfill the condition

$$\int_{\partial B} (\phi(\mathbf{r}') - \phi_\infty)\lambda(\mathbf{r}')dr' = 0, \tag{17}$$

where $\lambda(\mathbf{r}')$ is the solution to

$$\int_{\partial B} g(\mathbf{r},\mathbf{r}')\lambda(\mathbf{r}')dr' = 1; \qquad \mathbf{r} \in \partial B, \tag{18}$$

which is a FIE of the first kind.
The current density in B_e is calculated by differentiating equation (15), which result in

$$\nabla\phi(\mathbf{r}) = \int_{\partial B} \nabla\frac{\partial g(\mathbf{r},\mathbf{r}')}{\partial n'}\mu(\mathbf{r}')dr'; \qquad \mathbf{r} \in B_e. \tag{19}$$

With the source density $\mu(\mathbf{r}')$ known we may calculate the electric potential $V(\mathbf{r})$ utilizing equations (15) and (5) and the current density $\mathbf{J}(\mathbf{r})$ from equation (19) and (3). The normal current density on the surface is calculated just outside of ∂B using (19), utilizing that the normal current density is continuous across an interface.

3.5. Discretizing the integral equations

A general set of Lagrangian basis function of order M can represent a function F on a triangular element as [5]

$$F(L_1,L_2,L_3)=\sum_{i=0}^{M}\sum_{j=0}^{M-i}e_{ijk}Q_{ijk}(L_1,L_2,L_3);\qquad i+j+k=M\ , \tag{20}$$

where e_{ijk} is the value of F at the nodes. The basis functions have the following properties

$$\left.\begin{aligned}&Q_{ijk}(L_1,L_2,L_3)=R_i(M,L_1)R_j(M,L_2)R_k(M,L_3)\\&R_s(M,L)=\frac{1}{s!}\prod_{k=0}^{s-1}(ML-k);\qquad (s>0)\\&R_0(M,L)=1;\qquad\qquad (s=0)\end{aligned}\right\}. \tag{21}$$

For an isoparametric expansion the curvature is described as

$$\left.\begin{aligned}&\tilde{\boldsymbol{r}}=\sum_{i=0}^{M}\sum_{j=0}^{M-i}\boldsymbol{r}_{ijk}\,Q_{ijk}(L_1,L_2,L_3)\\&d\tilde{r}=\left|\det(\boldsymbol{J})\right|dL_1dL_2\end{aligned}\right., \tag{22}$$

where $\boldsymbol{r}_{ijk}$ is the coordinate of the appropriate node and $\boldsymbol{J}$ is the Jacobian. The unit normal vector is written as

$$\tilde{\mathrm{n}}=\frac{\det(\boldsymbol{J})}{\left|\det(\boldsymbol{J})\right|}, \tag{23}$$

pointing from the parametric surface $\partial\tilde{B}$ into the exterior domain B_e. From the discretization (20-23) we have that the integration of the surface ∂B yield

$$\left.\begin{aligned}&\int_{\partial B}g(\mathbf{r},\mathbf{r}')f(\mathbf{r}')dr'\approx\sum_{n=1}^{N}\sum_{i=0}^{M}\sum_{j=0}^{M-1}e_{\nu}\int_{\partial\tilde{B}_n}g(\mathbf{r},\tilde{\mathbf{r}}_n)Q_{ijk}(\mathbf{L})d\tilde{r}_n\\&\int_{\partial B}\frac{\partial g(\mathbf{r},\mathbf{r}')}{\partial n}f(\mathbf{r}')dr'\approx\sum_{n=1}^{N}\sum_{i=0}^{M}\sum_{j=0}^{M-1}e_{\nu}\int_{\partial\tilde{B}_n}\frac{\partial g(\mathbf{r},\tilde{\mathbf{r}}_n)}{\partial n}Q_{ijk}(\mathbf{L})d\tilde{r}_n\\&\int_{\partial B}\frac{\partial g(\mathbf{r},\mathbf{r}')}{\partial n'}f(\mathbf{r}')dr'\approx\sum_{n=1}^{N}\sum_{i=0}^{M}\sum_{j=0}^{M-1}e_{\nu}\int_{\partial\tilde{B}_n}\frac{\partial g(\mathbf{r},\tilde{\mathbf{r}}_n)}{\partial n'}Q_{ijk}(\mathbf{L})d\tilde{r}_n\end{aligned}\right\}, \tag{24}$$

assuming that the surface has been discretized into N faces and that we have a mesh dependent function *v(n,ijk)* that identify the collocation points given the face index *n* and the node index *ijk*. The numerical integration of each face is performed using a Gaussian quadrature rule for triangles.

3.6. Numerical implementation

Applying a collocation approach, where the collocation points in the simplex coordinate **L** is $\left\{\frac{i}{M},\frac{j}{M},\frac{k}{M}\right\}$, the basis function $Q_{ijk}(\mathbf{L})$ has unity value at node *ijk* and vanishes at every other node. Hence, the contribution from the singularities and the part $-\frac{1}{2}\gamma(\mathbf{r})$ and $+\frac{1}{2}\mu(\mathbf{r})$ in equation (14) and (16) will be added to the diagonal entries in the kernel matrix. In the Neumann case the kernel matrix is calculated as

$$\left.\begin{aligned} A_{p,v} &= \sum_{n=1}^{N}\sum_{i=0}^{M}\sum_{j=0}^{M-1}\int_{\partial\tilde{B}_n}\frac{\partial g(\mathbf{r},\tilde{\mathbf{r}}_n)}{\partial n}Q_{ijk}(\mathbf{L})d\tilde{r}_n \\ A_{qq} &= -\sum_{p}A_{pq}-1 \end{aligned}\right\}, \tag{25}$$

and in the Dirichlet case the kernel matrix is calculated as

$$\left.\begin{aligned} A_{p,v} &= \sum_{n=1}^{N}\sum_{i=0}^{M}\sum_{j=0}^{M-1}\int_{\partial\tilde{B}_n}\frac{\partial g(\mathbf{r},\tilde{\mathbf{r}}_n)}{\partial n'}Q_{ijk}(\mathbf{L})d\tilde{r}_n \\ A_{qq} &= -\sum_{p}A_{pq} \end{aligned}\right\}. \tag{26}$$

The singularities S_q in (25) and (26), which contribute to the diagonal entries, have been approximated by

$$S_q = -\tfrac{1}{2} - \sum_{p}A_{pq}\ , \tag{27}$$

using that $\sum Q_{ijk}(\mathbf{L}) = 1$ and that $\int_{\partial B}\frac{\partial g(\mathbf{r},\tilde{\mathbf{r}}_n)}{\partial n'}dr' = -\frac{1}{2}$ when $\mathbf{r}\in\partial B$.
We end up with a system of linear equations

$$\mathbf{A}(\mathbf{r},\mathbf{r}')\mathbf{x}(\mathbf{r}') = \mathbf{b}(\mathbf{r}), \tag{28}$$

where $\mathbf{A}(\mathbf{r},\mathbf{r}')$ is the kernel matrix, $\mathbf{b}(\mathbf{r})$ is the boundary condition at $\mathbf{r}$ and $\mathbf{x}(\mathbf{r}')$ is the coefficients to the set of Lagrange basis functions (20) and also the solution to the integral equations (14) and (16).

4. Numerical validation

We have chosen to validate our code against a known analytical solution in the Dirichlet case, where we will show the convergence of the solutions as a function of the surface discretization. We will also do a comparison with a commercial code on a more complicated geometry. In these examples we have chosen the conductivity $\sigma = 1$ S/m and thus the current potential $\phi(\mathbf{r})$ has the same amplitude as the electric potential $V(\mathbf{r})$.

4.1 Analytical validation

Given the potential on the surface of a sphere, the potential in the exterior to that sphere could be calculated analytically by means of multipole technique. A relevant problem is that of two different potentials, corresponding to two non-polarizable materials with different electrochemical potential next to each other. Assuming the origin at the center of a sphere with radius $R = 8\,\mathrm{m}$, the boundary condition yielding

$$V(\mathbf{r}) = \begin{cases} -0.8\,\mathrm{V} & z < 0 \\ -0.2\,\mathrm{V} & z > 0 \end{cases}. \tag{29}$$

The electric infinity potential is thus $V_\infty = -0.5\,\mathrm{V}$. Spheres with different number of faces are created in order to study the convergence of the solution. Here we have approximated the sphere with 8, 32 and 144 faces.

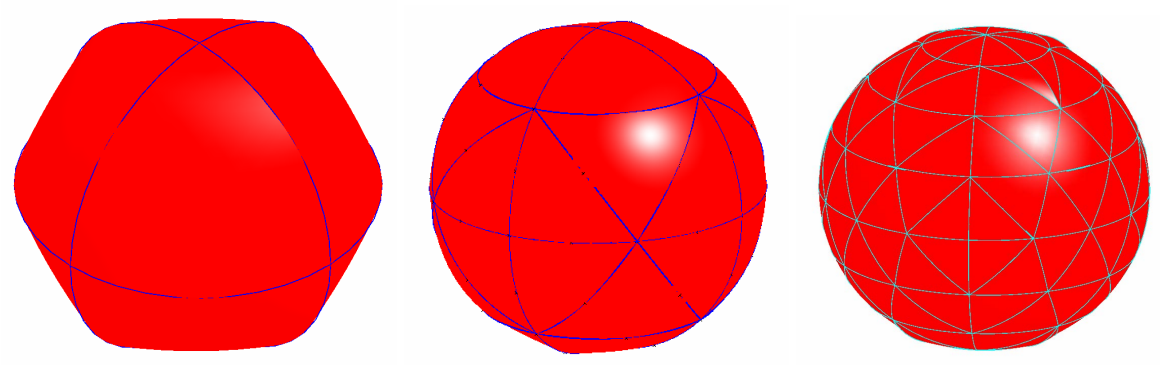

Figure 2. Spheres consisting of 8, 32 and 144 faces used to study the convergence of the solution compared to the known analytical.

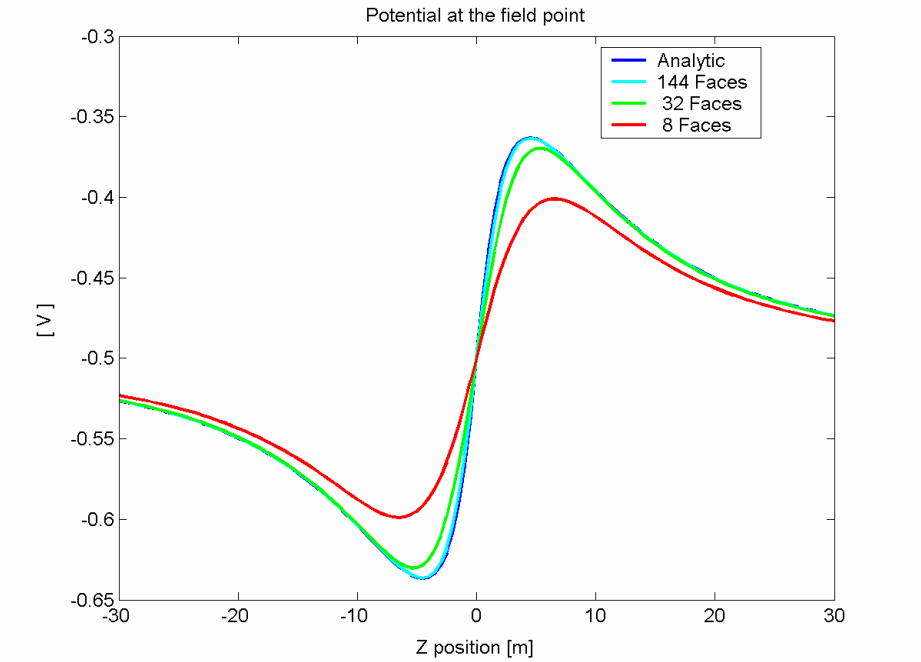

Figure 3. The electric potential at the field point applying the Dirichlet boundary condition.

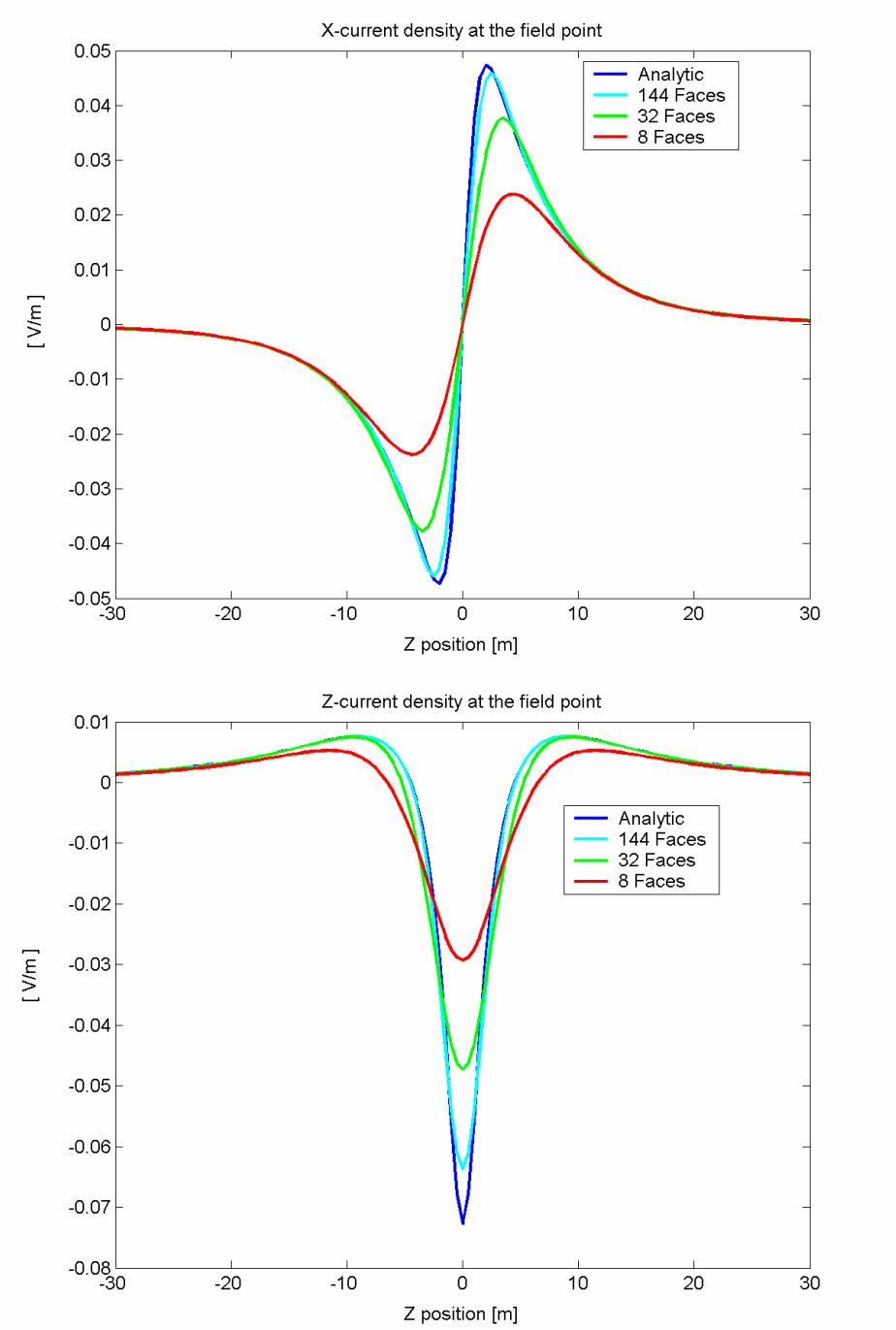

Figure 4. The current density at the field point applying the Dirichlet boundary condition.

The solutions are validated on a line where z varies between $-30\,\mathrm{m}$ and $30\,\mathrm{m}$ and $x = 10\,\mathrm{m}$ and $y = 0\,\mathrm{m}$. We can see from figure 3 how the solution converges toward the analytical solution. Already for the 8 faces solution we obtain $V_\infty = -0.5\,\mathrm{V}$ with high accuracy. Figure 4 further enhance the convergence of the solution, where the differences in current density will vanish as the mesh around $z = 0$ (the discontinuity) is further refined.

4.2 Boundary element codes comparison

In order to test the solution on a more complicated geometry, we have to compare our code with an existing commercial. We have created the model in the commercial program and exported that geometry to our code.

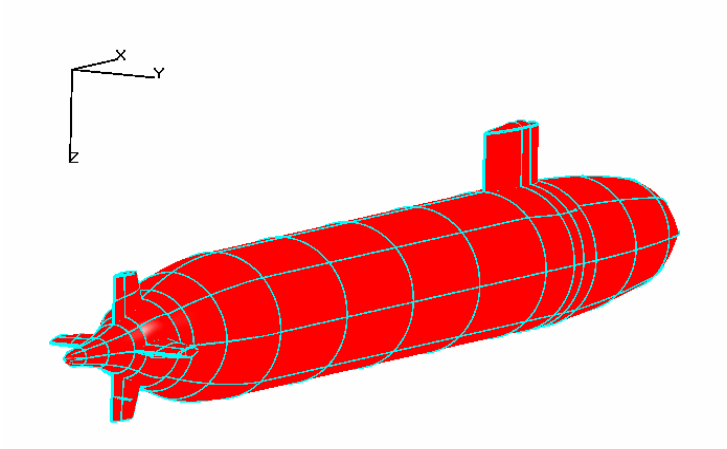

Figure 5. A scale model of a submarine with length 0.9m*, where the hull is given an electric potential of* $-0.8\,\text{V}$ *and the area at the stern is given an electric potential of* $-0.2\,\text{V}$.

The electric potential and the current density are calculated along a line straight beneath the submarine model. The obtained results are shown in figures 6-7.

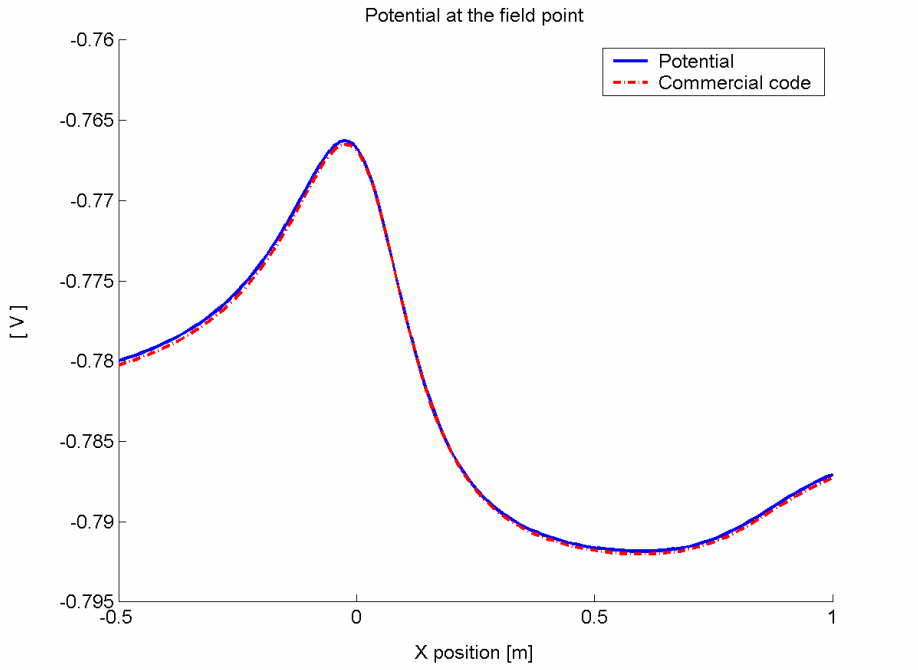

Figure 6. The potential $V(\mathbf{r})$ *along a line straight beneath the submarine model. The blue line shows the potential from our code and the dashed red line shows the potential obtained from the commercial code.*

The potentials have similar appearance, as shown in figure 6. The solution of $(\phi(\mathbf{r})-\phi_\infty)$, obtained from solving (16), is about the same as the solution from the commercial code, whereas the ϕ_∞ contribution, from the solution of (17-18), differs slightly, i.e. our code has calculated $\phi_\infty = -0.7832$ A/m, and the commercial code has calculated $\phi_\infty = -0.7835$ A/m.

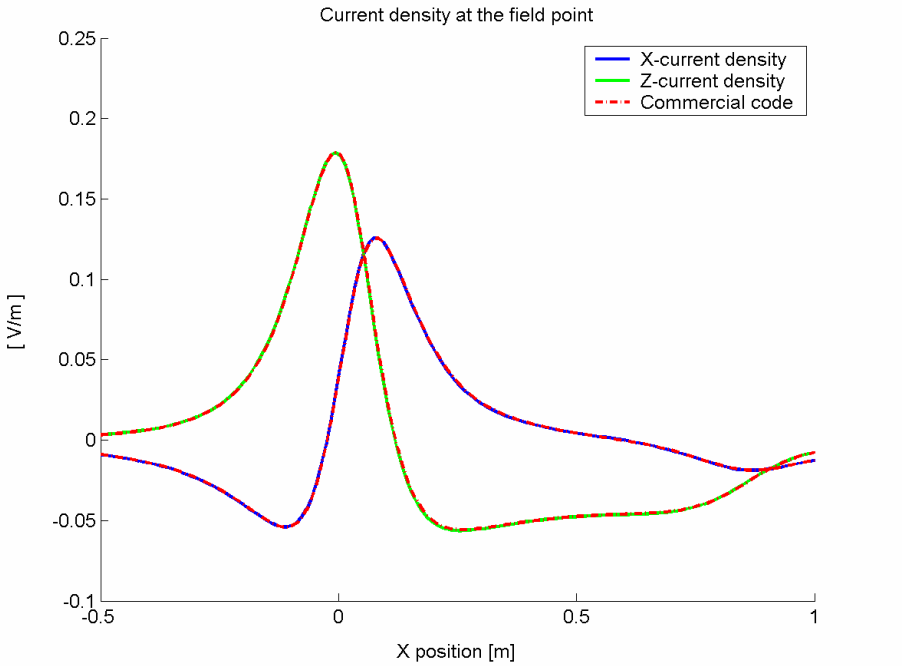

Figure 7. The current densities along a line straight beneath the submarine. The blue and the green line show the x-current density and the z-current density from our code. The dashed red lines show the results from the commercial code.

The current density solution is almost identical as a result of the good coherence between the solutions of $(\phi(\mathbf{r})-\phi_\infty)$ for our and the commercial code.

The Neumann case is considered to be validated as the Dirichlet case is validated. The kernel in the Neumann case is the transpose of the Dirichlet matrix (10), which we have validated and the singular contribution is the same (27). The calculation of ϕ_∞ is performed separately and does not effect the Neumann solution.

5. Discussion

The relatively good accuracy that we have seen will probably be enough for our applications. However, it is straightforward to enhance the code to higher order polynomial expansion. For quadrilateral faces a little work has to be done.

With full control over the forward model, the work with the inverse solvers and regulators to controlling the corrosion and the electric signature will be simplified. The created interface with the commercial boundary element code will also be useful in further evaluations and researches.

References

[1] H. Claésson, A. Brage, “Verifiering av SE-signaturmodeller”, FOI-R-0955-SE, 2003

[2] M. A. Jaswon, G. T. Symm, “Integral Equation Methods in Potential Theory and Elastostatics”, Academic Press, 1977

[3] N. Morita, N. Kumagai, J.R. Mautz, “Integral Equation Methods for Electromagnetics”, Artech House, 1990

[4] I. Stakgold, “Green´s Functions and Boundary Value Problems”, John Wiley & Sons, 1979

[5] A. F. Peterson, S. L. Ray, R. Mittra, “Computational Methods for Electromagnetics”, IEEE Press, 1998

[6] J.D. Jackson, “Classical Electrodynamics”, John Wiley & Sons, 1975